

TEMPERATURE-DEPENDENT STUDY OF RAMAN SPECTRA OF $\text{Cu}_2\text{ZnSnSe}_4$ SINGLE CRYSTALS

V.F. GREMENOK^{1,2}, V.V. KHOROSHKO², T.N. OSMOLOVSKAYA²,
N.N. MUSAYEVA³, B.M. IZZATOV³

¹*Scientific-Practical Materials Research Centre of the National Academy of Sciences of
Belarus, Minsk, Republic of Belarus, 220072, P. Brovka str. 19*

²*Belarusian State University of Informatics and Radioelectronics,
Minsk, Republic of Belarus, 220013, P. Brovka str., 6*

³*Institute of Physics, ANAS, Baku, Azerbaijan, AZ1143, H. Javid ave., 131*

e-mail: nmusayeva@physics.science.az ; tel: (012)5393259; mob:0503025647

Single crystals of $\text{Cu}_2\text{ZnSnSe}_4$ (CZTSe) were grown by chemical vapor transport using iodine as a transport agent. Temperature dependence of the Raman active modes for crystals in the temperature range of 24–290 K have been investigated. X-ray phases analysis shows the presence of CZTSe tetragonal phase. Analysis of the experimental spectra has permitted identification of 9 peaks, which positions are in good accord with theoretical predictions. It is shown that the shift of the Raman peaks with temperature may be associated with thermal expansion, while the broadening is mainly determined by the phonon damping processes in this material. It is established that dimensionality is a key factor in regulating the dominant phonon decay mechanism.

Keywords: kesterite, $\text{Cu}_2\text{ZnSnSe}_4$, Raman spectra, Temperature dependence.

PACS: 72.40.+w, 78.30.Hv

Earth abundant quaternary semiconductor $\text{Cu}_2\text{ZnSnSe}_4$ (CZTSe) have been intensively studied because of their desired optoelectronic properties for photovoltaic (PV) applications. The best solar cell efficiency has reached values of 12.6% for alloyed kesterite (CZTSSe) photovoltaic devices [1]. In order to achieve an increase in the efficiency, problems involving material require for an accurate control of the microstructure of the kesterite absorbers. Raman spectroscopy has big potential in the analysis of crystal structure. Temperature-dependent Raman investigations have already been reported for various semiconducting materials including copper indium selenide (CIS) thin films, gallium arsenide, and silicon [2]. This work presents the temperature dependence of the Raman peaks position for $\text{Cu}_2\text{ZnSnSe}_4$ crystals in the temperature range of 24–290 K.

Single crystals of CZTSe were grown by chemical vapor transport using iodine as a transport agent. Samples were synthesized from the elements (Alfa Aesar: Cu - 3N, Zn - 5N, Sn - 3N and Se - 5N purity) in stoichiometric proportions. The composition of the grown crystals was determined using X-ray microprobe analysis. An AVALON-8000 X-ray spectrometer was used as an X-ray spectrum analyzer. Analysis of the phase composition was performed with the use of the Crystallography Open Database (COD) by «Match» software package [3]. The temperature-dependent Raman measurements at ambient pressure were conducted using a Horiba Jobin Yvon LabRam HR800 VIS single-stage Raman spectrometer, equipped with 1800 L/mm diffraction grating and a Peltier-cooled charged-coupled device (CCD). A solid-state laser ($\lambda = 532$ nm) served as the laser excitation source. The sample was placed in a vacuum temperature-controlled cell (pressure less than

5×10^{-4} Pa, temperature setting accuracy of 0.05 K). The Raman-relevant parameters were obtained from the fitting of the Raman spectra with Lorentzian functions, accompanied by linear background correction/subtraction.

The elemental composition of the CZTSe crystals is represented in Table 1. The ratios of Cu/(Zn+Sn) indicated a small excess of copper in the samples. The results of X-ray microanalysis of the grown $\text{Cu}_2\text{ZnSnSe}_4$ single crystals are in satisfactory agreement with a given composition in the initial charge.

The powder XRD patterns of crystals exhibit major peaks corresponding to diffraction lines of the Kesterite structure of CZTSe (ICDD data #00-052-0868). No distinct peaks of secondary phases are observed in the XRD pattern. The XRD analysis demonstrates that the samples mainly consists of CZTSe tetragonal phase ($2\theta = 27.2^\circ$ (112), 30.9° (200), 45.2° (204), 53.5° (312) and 65.8° (008)). The full-width at half-maximum (FWHM) of the (112) peak of CZTSe is 0.091. The lattice constants of a- and c-axes in the CZTSe crystals were calculated from the XRD patterns. These values correspond well to reported values of CZTSe ($a = 5.693$ Å, $c = 11.333$ Å) [4].

It is difficult to investigate single phase from XRD measurement because the peaks of CZTSe almost corresponded to those of ZnSe and Cu_2Se [5]. Hence, Raman spectroscopy is useful to investigate the structure and phase purity of CZTSe material besides XRD. Raman spectra of $\text{Cu}_2\text{ZnSnSe}_4$ crystals in the range of 50–250 cm^{-1} are shown in Fig. 1. The peak positions at room temperature matches well with previously published results for kesterite phase of CZTSe (Table 2) [5 - 8].

Table 1.

The elemental composition and atomic ratios of the CZTSe single crystals.

Atomic percent				Ratio				
Cu	Zn	Sn	Se	Zn/Sn	Cu/Zn	Cu/Sn	Cu/(Zn+Sn)	Se/metal
25.97	12.48	11.61	49.94	1.07	2.08	2.23	1.08	0.99

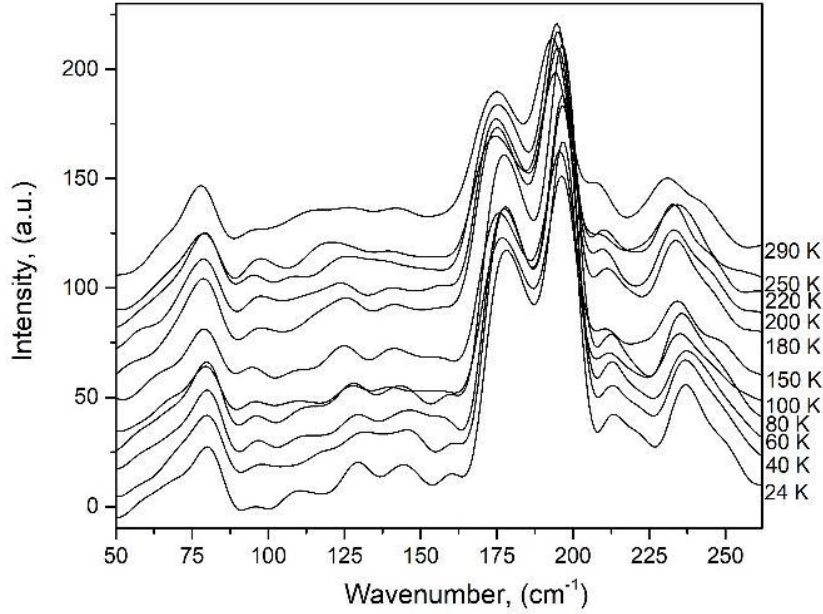


Fig. 1. Raman spectra of CZTSe single crystals recorded at various temperatures.

Table 2.

Frequency (in cm^{-1}) of peaks from simultaneous fitting of Raman spectra for CZTSe crystals measured at 290 K with excitation wavelength of 523 nm.

Peak position, cm^{-1}	Phase	Symmetry	References
76	CZTSe	E (TO LO)	[5 – 7]
97	CZTSe	B (TO LO)	[5 – 7]
118	SnSe ₂		[8]
142	CZTSe	E (TO LO)	[5 – 7]
174	CZTSe	A ²	[5 – 7]
193	CZTSe	A ¹	[5 – 7]
209	CZTSe	A	[5 – 7]
230	CZTSe	B (TO LO)	[5 – 7]
243	CZTSe	B (TO LO)	[5 – 7]

For precise determination of the FWHM and peak positions, we used peak approximation with a single Lorentz function for each temperature point. The temperature dependencies of FWHM and peak position were analyzed by the approximation with the linear model and the Klemens model [9]. For a detailed analysis of the Raman spectra for CZTSe crystals obtained at different temperatures, we focus on the two Raman modes with A-symmetry labelled as A¹ and A². A decrease in the frequency and intensity of modes is observed with an increase in temperature. An increase in linewidth/damping is also observed with increase in temperature. It was revealed that the temperature dependencies of Raman shift and FWHM of CZTSe crystals have non-linear character, as these

dependencies are better approximated with the Klemens model than with the linear one. The same effects were observed for Cu₂ZnSnS₄ films [9].

We acquired the individual contributions to each Raman mode, namely, the thermal expansion and anharmonic interactions terms responsible for the Raman shift and broadening with temperature. Our results indicate that the Raman shift with temperature is dominated by the thermal expansion term, whereas the broadening is mainly governed by three-phonon damping processes in this material. Considering relevant results from the literature, it appears that dimensionality is a key factor in regulating the dominant phonon decay mechanism.

The analysis of Raman data showed that the phonon damping process is the main factor responsible for the observed frequency shift as well as for the linewidth variation. The results indicate the significant role of dimensionality in determining the dominant phonon damping factor, thus opening the

way for tuning the physical properties of this class of materials by appropriate growth conditions.

The part of the work was financed by the Belarusian State Programme for Research «Physical Material Science, New Materials and Technologies».

-
- [1] D.H. Son, S.H. Kim, S.Y. Kim, Y.I. Kim, J.H. Sim, S.N. Park, D.H. Jeon, D.K. Hwang, S.J. Sung, J.K. Kang, D.H. Kim. Effect of solid- H_2S gas reactions on CZTSSe thin film growth and photovoltaic properties of a 12.62% efficiency device. *J. Mater. Chem.* 2019, Vol. A 7 (44), P. 25279 - 25289.
- [2] B. Schrader. *Infrared and Raman Spectroscopy*. VCH Publishers, New York, 1995, 414 p.
- [3] L. Lutterotti, S. Matthies, H.R. Wenk. MAUD (Material Analysis Using Diffraction): a user friendly Java program for Rietveld Texture Analysis and more. *Proceedings of the 12th International Conference on Textures of Materials (ICOTOM-12)*, 1999, Vol. 1, P. 1599.
- [4] V.F. Gremenok, V. G. Gurtovoi, A.V. Stanchik, T.V. Shelkovaya, V.A. Chumak, E.V. Rabenok, V.V. Rakitin, B.I. Golovanov and G.F. Novikov. Polycrystalline $\text{Cu}_2\text{ZnSn}(\text{S}_x\text{Se}_{1-x})_4$ Solid Solutions: Synthesis, Phase Composition, and Photoconductivity Decay Kinetics. *Inorganic Materials*, 2020, Vol. 56, № 10, P. 1000 - 1005.
- [5] T. Gürel, C. Semik, T. Cagin. Characterization of vibrational and mechanical properties of quaternary compounds $\text{Cu}_2\text{ZnSnS}_4$ and $\text{Cu}_2\text{ZnSnSe}_4$ in kesterite and stannite structures. *Phys. Rev.*, 2011, Vol. B 84, P. 205201 (7).
- [6] M. Dimitrievska, H. Xie, A. Fairbrother, X. Fontané, G. Gurieva, E. Saucedo, Al. Pérez-Rodríguez, S. Schorr and V. Izquierdo-Roca. Multiwavelength excitation Raman scattering of $\text{Cu}_2\text{ZnSn}(\text{S}_x\text{Se}_{1-x})_4$ ($0 \leq x \leq 1$) polycrystalline thin films: Vibrational properties of sulfoselenide solid solutions. *Appl. Phys. Lett.*, 2014, Vol. 105, P. 031913 (5).
- [7] Ankur Khare, Burak Himmetoglu, Melissa Johnson, David J. Norris, Matteo Cococcioni, Eray S. Aydil. Calculation of the lattice dynamics and Raman spectra of copper zinc tin chalcogenides and comparison to experiments. *J. Appl. Phys.*, 2012, Vol. 111, 083707 (9).
- [8] Pedro M. P. Salome, Paulo A. Fernandes, Joaquim P. Leitao, Marta G. Sousa, Jennifer P. Teixeira, Antonio F. da Cunha. Secondary crystalline phases identification in $\text{Cu}_2\text{ZnSnSe}_4$ thin films: contributions from Raman scattering and photoluminescence, *J Mater Sci*, 2014, Vol. 49, P. 7425 - 7436.
- [9] D. Lu, S. Luo, S. Liu, H. Yao, X. Ren, W. Zhou, D. Tang, X. Qi, J. Zhong. Anomalous Temperature-dependent Raman Scattering of Vapor Deposited 2D Bi Thin Films. *J. Phys. Chem. C*, 2018, Vol. 122, P. 24459 - 24466.